Carbon Nanotubes and Carbon Nanofibers for Enhancing the Mechanical Properties of Nanocomposite Cementitious Materials

Bryan M. Tyson, S.M.ASCE[1]; Rashid K. Abu Al-Rub, M.ASCE[2]; Ardavan Yazdanbakhsh, S.M.ASCE[3]; and Zachary Grasley, M.ASCE[4]

Abstract: Carbon nanotubes (CNTs) and carbon nanofibers (CNFs) are quickly becoming two of the most promising nanomaterials because of their unique mechanical properties. The size and aspect ratio of CNFs and CNTs mean that they can be distributed on a much finer scale than commonly used microreinforcing fibers. As a result, microcracks are interrupted much more quickly during propagation in a nano-reinforced matrix, producing much smaller crack widths at the point of first contact between the moving crack front and the reinforcement. In this study, untreated CNTs and CNFs are added to cement matrix composites in concentrations of 0.1 and 0.2% by weight of cement. The nanofilaments are dispersed by using an ultrasonic mixer and then cast into molds. Each specimen is tested in a custom-made three-point flexural test fixture to record its mechanical properties; namely, the Young's modulus, flexural strength, ultimate strain capacity, and fracture toughness, at 7, 14, and 28 days. A scanning electron microscope (SEM) is used to discern the difference between crack bridging and fiber pullout. Test results show that the strength, ductility, and fracture toughness can be improved with the addition of low concentrations of either CNTs or CNFs. **DOI: 10.1061/(ASCE)MT.1943-5533.0000266.**

CE Database subject headings: Cement; Dispersion; Bonding; Ductility; Nanotechnology.

Author keywords: Carbon nanotubes; Carbon nanofibers; Cement; Dispersion; Bond; Strength; Ductility.

Introduction

Concrete is the most commonly and widely used construction material in the world. However, cementitious materials in general, are very brittle and characterized by a very low tensile strength and strain capacity. Macroscopic steel reinforcing bars are added to provide tensile strength and ductility. Within the last few decades, researchers started testing discrete macro- to microfibers to control crack growth in cementitious materials (e.g., cement paste, cement grout, concrete) (Altoubat et al. 2009; Fischer and Li 2007; Li and Maalej 1996; Mangat et al. 1984; Ostertag et al. 2001; Savastano et al. 2005; Wang et al. 2008). The idea behind this transition to fiber reinforced concrete (FRC) is that the tensile strength is developed from many individual fibers rather than a few pieces of steel (Altoubat et al. 2009). Therefore, the use of discrete fibers results in a more uniform distribution of stress within the matrix. Recently, exceptional types of carbon nanofilaments have raised the interest of some concrete researchers because of their remarkable mechanical, chemical, electrical, and thermal properties, and excellent performance in reinforcing polymer-based materials (Coleman et al. 2006; Marrs et al. 2007; Wang et al. 2006a). Microfibers may delay the nucleation and growth of cracks at the microscale, whereas nanoreinforcements will further delay the nucleation and growth of cracks at the nanoscale and stop their propagation to the microlevel. These nanofilaments, both carbon nanotubes (CNTs) and carbon nanofibers (CNFs), may prove to be superior alternatives or complements to traditional fibers and promising candidates for the next generation of high-performance and multifunctional cement-based materials and structures.

Experimental tests on CNFs have shown them to have a Young's Modulus as high as 400 GPa, with a tensile strength of 7 GPa (Zhou et al. 2009). Alternatively, CNTs have an average Young's modulus around 1 TPa, a tensile strength of 60 GPa, and an ultimate strain of 12% (Yu et al. 2000). As a result, CNTs are quickly becoming one of the most promising nanomaterials because of their unique mechanical properties. Compared to steel, CNTs have a modulus of elasticity approximately 5 times higher, a tensile strength 100 times larger, can reach elastic strain capacities 60 times greater than steel, and yet have a specific gravity one sixth that of steel. Moreover, CNTs occur as single-walled carbon nanotubes (SWCNTs) and multiwalled carbon nanotubes (MWCNTs). SWCNTs are composed of a single graphene sheet rolled into a long hollow cylinder, whereas MWCNTs (and also CNFs) are nested arrays of graphene.

The superior mechanical properties of the CNFs and CNTs alone do not ensure mechanically superior nanocomposite cement. The properties of the nanocomposite are strongly influenced by two primary factors. The first is the dispersion of nano-filaments within the cementitious matrix. The other is the bond strength and energy between the matrix and surface of the CNT or CNF. Because of high van der Waals forces, carbon nanofilaments are strongly

[1]Graduate Student, Zachary Dept. of Civil Engineering, Texas A&M Univ., College Station, TX 77843.

[2]Assistant Professor, Zachary Dept. of Civil Engineering, Texas A&M Univ., College Station, TX 77843 (corresponding author). E-mail: rabualrub@civil.tamu.edu

[3]Graduate Student, Zachary Dept. of Civil Engineering, Texas A&M Univ., College Station, TX 77843.

[4]Assistant Professor, Zachary Dept. of Civil Engineering, Texas A&M Univ., College Station, TX 77843.

Note. This manuscript was submitted on June 29, 2010; approved on January 5, 2011; published online on January 7, 2011. Discussion period open until December 1, 2011; separate discussions must be submitted for individual papers. This paper is part of the ***Journal of Materials in Civil Engineering***, Vol. 23, No. 7, July 1, 2011. ©ASCE, ISSN 0899-1561/2011/7-1028–1035/$25.00.

attracted to one another. However, one can expect CNTs to be affected more by van der Waals forces than CNFs because of their larger surface-area-to-volume ratio. This higher attraction causes the CNTs to be more prone to agglomeration (bundling). This attraction causes them to rapidly settle out of suspension if not properly treated with surfactants and mixed with an ultrasonic mixer. (An ultrasonic mixer is a device that uses a high frequency driver to transmit acoustical energy throughout a liquid medium.) The energy in the shock waves is extremely high, significantly accelerates chemical reactions, and breaks the clumps and agglomerations of particles. Although previous research has shown successful results in dispersing both CNTs and CNFs within aqueous solutions (Chen et al. 2006; Grunlan et al. 2008; Xie et al. 2005), few of these techniques can be applied to cementitious materials because of the retarded (i.e., delayed) hydration of the cement paste caused by large quantities of surfactants (Cwirzen et al. 2008).

For dispersing CNTs in aqueous solutions, Wang et al. (2006b) used a microwave to functionalize SWCNTs in a solution of nitric and sulfuric acid. Grunlan et al. (2008) conducted research on the use of polyacrylic acid (PAA) and polyallylamine hydrochloride (PAH) as a means to control the dispersion of nonfunctionalized carbon nanotubes based on the pH of the solution. The grafting of polymers to the nanotubes was successfully demonstrated by Zhao et al. (2005). These solutions were capable of reaching aqueous concentrations as high as 5 mg/ml. Bandyopadhyaya et al. (2002) were able to disperse up to 15 wt% (i.e., by weight of water) CNTs into an aqueous solution containing gum arabic and mixing for 20 min with an ultrasonic mixer. These techniques have been, to a reasonable extent, successful in dispersing CNTs in polymeric materials. However, these techniques may not always be appropriate for cementitious materials.

Whereas considerable research on CNTs and CNFs has been focused on their incorporation within polymers, very little attention has been focused on combining CNTs or CNFs with cement. Therefore, the research on the integration of CNTs and CNFs in cementitious materials is at a relatively novel stage; very limited research regarding their effectiveness in enhancing the flexural strength or toughness of concrete has been conducted. Within the area of dispersion techniques applicable to cementitious materials, Makar and Beaudoin (2004) and Makar et al. (2005) made cement paste containing between 1.6 and 2 wt% of SWCNT-coated cement. However, they did not report any mechanical testing. Within the last few years, researchers have performed different mechanical tests on cement samples by varying concentrations of CNT between 0.02 and 0.5 wt% by weight of cement (Cwirzen et al. 2008; Li et al. 2005; Li et al. 2007; Musso et al. 2009; Sáez de Ibarra et al. 2006; Wansom et al. 2006). Only a small number of studies on CNT reinforced cementitious composites contain results from multiple ages, and none discuss properties such as peak displacement at fracture or fracture toughness. Most researchers focus on the compressive of splitting tensile strength. Very little work has been done on flexural strength of nanocomposite cementitious materials (Li et al. 2005; Shah et al. 2009).

As far as the integration of CNFs in cementitious materials, even fewer studies have been conducted than to that of CNTs. Recently, Sanchez (2009) studied the effect of CNFs on the mechanical properties. Despite the efforts made to date in integrating CNTs and CNFs in cementitious materials, only marginal success has been realized, and the objective of this study is to address this issue.

In this study, cement paste is reinforced with low concentrations of either CNFs or MWCNTs at either 0.1 wt% or 0.2 wt% (by weight of cement). To aid in the creation of a uniform dispersion, the as-received nanofilaments are first dispersed in an aqueous solution along with a commercially available surfactant by using an ultrasonic mixer. The mechanical properties of the specimens are measured with a custom-built three-point flexural test fixture at 7, 14, and 28 days. Four major mechanical properties are determined for each test: ultimate strength, ultimate strain capacity, elastic modulus, and fracture toughness. To the writers' knowledge, this study is the first to date that presents data for the four major mechanical properties at multiple days. A scanning electron microscope (SEM) is used to observe the fractured surface of the samples to understand how the concentration of the nanofilaments affects the mechanical properties of the nanocomposite cement paste.

Experimental Setup

Materials

The cement used for the tests is a commercially available Type I/II portland cement. The CNFs (Pyrograf III, Applied Sciences, Cedarville, OH) were factory treated to remove any remaining polyaromatic hydrocarbons from the surface. The CNFs have a diameter ranging from 60 to 150 nm, and a length of 30 to 100 μm. The CNFs have an aspect ratio (i.e., length to diameter) as high as 1,500. Table 1 summarizes the physical properties of the CNFs. The CNTs were MWCNTs (NC7000, Nanocyl, Sambreville Belgium) and were produced by a catalytic carbon vapor deposition (CCVD) process. They have a well-controlled diameter of 9.5 nm and an average length of 1.5 μm, with an aspect ratio of 150. The properties of the CNTs are also listed in Table 1. The CNTs and CNFs were used as received from the manufacturer without any surface functionalization. Previous research (Yazdanbakhsh et al. 2009) has shown that a high-range polycarboxylate-based water reducing admixture commercial superplasticizer (ADVA Cast 575, Grace Corporation, Cambridge, MA) works well to disperse the CNTs or CNFs with minimal effects on the hydration time.

Preparation and Testing

Five batches of cement paste were produced. These included a reference sample of plain cement paste, two batches of cement paste with CNTs at 0.1 wt% and 0.2 wt% by weight of dry cement, and two batches with CNFs at 0.1 wt% and 0.2 wt%. Table 2 summarizes the composition of the five batches. These batches were labeled to indicate the components and their concentrations. The letter "F" represents CNFs, "T" represents CNTs, and "1" and "2" indicate filament dosages of 0.1 wt% and 0.2 wt%, respectively.

Table 1. Physical Properties of CNTs and CNFs

	CNFs	CNTs
Diameter	60–150 nm	9.5 nm
Length	30–100 μm	1.5 μm
Specific surface area	50–60 m^2/g	250–300 m^2/g
Purity	$\geq$ 90%	$\geq$ 90%

Table 2. Mix Design of the Test Specimens

Test specimens	Water/cement ratio	CNFs:% weight of cement	CNTs:% weight of cement
Reference	0.4	0	0
F1	0.4	0.1	0
F2	0.4	0.2	0
T1	0.4	0	0.1
T2	0.4	0	0.2

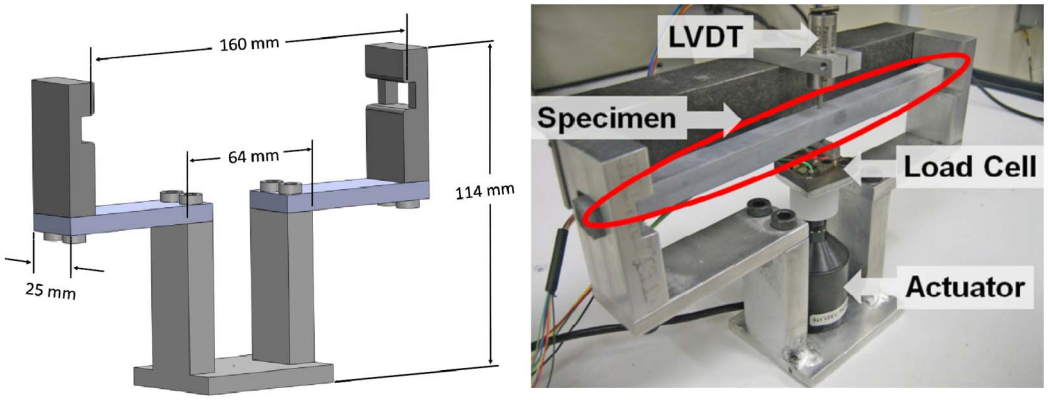

(a) (b)

Fig. 1. (a) 3D model of flexural load frame model; (b) test frame setup for three-point bend with cement specimen in place (Image by Bryan Tyson)

All five batches had a water to cement ratio of 0.40, and the batches containing CNTs or CNFs had a surfactant (i.e., superplasticizer) to cement ratio of 0.005. No surfactant was used in the plain cement samples. Three replications were made for each nanocomposite tested.

The nano-filaments were first dispersed within the aqueous solution by combining the water, surfactant, and either CNTs or CNFs. A liquid processor ultrasonic mixer (Vibra-Cell, model VC-505, Sonics & Materials, Newtown, CT) was used to disperse the nanofilaments. The CNFs were sonicated for 15 min, and the CNTs were sonicated for 30 min. These were the times needed to achieve well-dispersed CNFs and CNTs in the aqueous solution (Yazdanbakhsh et al. 2009). After sonication, the dispersed solution was then combined with the dry cement and mixed with a multispeed planetary mixer for 7 min to enhance the uniformity of the paste. After mixing, the cement paste was placed within a vacuum chamber for 3 min to remove any entrained air caused by the mixing process. Next, the cement paste was poured into square acrylic tubes with an internal cross-sectional area of 6.5 × 6.5 mm and an electric vibrator was used to ensure a uniform pour. All samples were demolded after 24 h and then cured in lime saturated water.

Testing Fixture

For the flexural testing of these small-scale specimens, a testing fixture was made that is capable of performing a three-point flexural test. The fixture was constructed out of aluminum and has a span length of 160 mm. The specimen holders were machined with a radius of 1.5 mm to reduce the stress concentrations caused by sharp corners. To minimize initial damage to the specimens before testing, one end of the fixture has a hole all the way through to allow the specimens to slide in without the need to cut the specimens after demolding. A 3D model of the test fixture (Fig. 1) shows the test frame, an actuator, a load cell, a linear voltage displacement transducer (LVDT), and a cement beam.

All data from the load cell and LVDT were recorded with a data acquisition board (National Instruments, Austin, TX). Programming was done within LabVIEW to automatically control the actuator and record displacement and force to a file. The force and displacement were converted to stress and strain by using simple strength of materials relations for a three-point bending beam such that

$$\sigma = \frac{3PL}{2bd^2}$$

and

$$\varepsilon = \frac{6Dd}{L^2}$$

where P = force from the load cell; L = span length (160 mm); b and d = width and depth (6.5 mm each); and D = displacement from the LVDT.

An SEM was used to observe the dispersion and bonding properties between the nanofilaments and the cement paste. An ultra high resolution field emission scanning electron microscope (FE-SEM) (JSM-7500F, JEOL, Tokyo) was used to observe the fracture surface of the samples. After the samples had been tested, the fracture surface was cut into an approximately 1 × 1 × 0.5 mm sample and coated with a 3 nm thick platinum/palladium layer to enhance surface conductivity. To reduce surface charging, all images used an acceleration voltage of 6 kV.

Results and Discussion

Aqueous Dispersion

To study the effects of ultrasonic mixing, different aqueous solutions were made with either CNFs or CNTs, and the sonication time was adjusted accordingly. The effect of ultrasonic mixing on the dispersion of CNFs is shown in Fig. 2. Fig. 2 is an optical

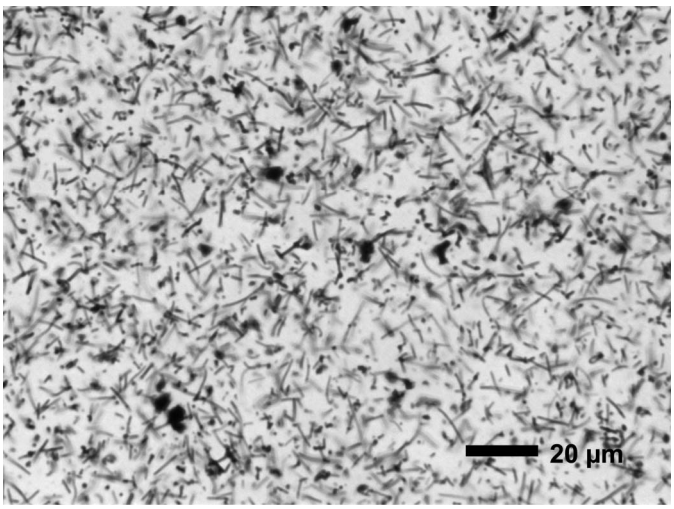

Fig. 2. Effect of ultrasonic mixing on the dispersion of CNFs in an aqueous solution containing a surfactant and sonicated for 15 minutes

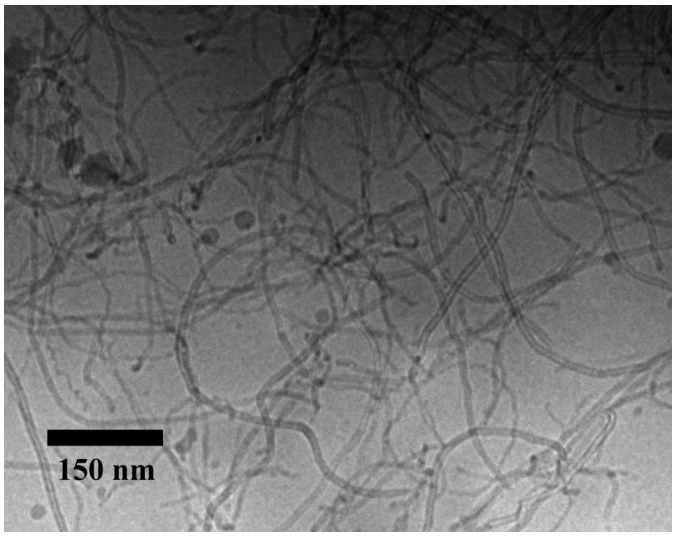

Fig. 3. Cryo-TEM image of CNTs dispersed in an aqueous solution; the small dark circles indicate the presence of impurities within the solution; many of the CNTs look to be intact, indicating ultrasonic mixing did not adversely affect the CNTs

microscopy image of an aqueous solution containing 0.25 wt% CNFs and 1.25 wt% of surfactant by weight of water that was sonicated for 15 min. The absence of large dark spots indicates that the solution is well dispersed. The few small dark spots are caused by impurities within the solution. The reduction in agglomerations is beneficial to the success of creating a well-dispersed solution of CNFs; however, the use of ultrasonic mixing should be controlled and optimized to reduce fiber breakage.

Fig. 3 shows the cryo-transmission electron microscope (TEM) image of CNTs dispersed in water containing 0.25 wt% CNTs and 1.25 wt% of surfactant by weight of water. The solution was mixed for 30 min by ultrasonication before cryogenic freezing in liquid nitrogen. Although the solution is not uniform across the entire image, the image does not include bundles of CNTs. The dispersion of CNTs is more difficult to optimize than CNFs. The amount of energy required to disperse CNTs is so high that some CNTs will break in the process.

Mechanical Properties

Fig. 4 shows the displacement at failure (i.e., peak displacement) for each batch at 7, 14, and 28 days. In Figs. 4–7, the bar represents the mean value, and the top and bottom error bars represent the third and first quartile, respectively. The addition of both CNTs and CNFs improves the peak displacement of cement paste. The greatest increase in peak displacement occurs with the addition of CNFs. A maximum increase of 150% was observed when using a concentration of 0.2 wt% CNFs. For the displacement at failure, both concentrations of CNFs outperformed CNTs. This is most likely attributed to the higher aspect ratios of the CNFs (i.e., approximately 1,000 for CNFs; 150 for CNTs), which makes CNFs more effective as reinforcements because of their larger interaction with the cement matrix. Another reason for the CNFs to outperform the CNTs is the enhanced dispersion achieved when using the CNFs.

The average peak stress (i.e., average flexural strength) results are shown in Fig. 5. The largest increase of 82% is found at 7 days for CNFs. In many cases, the addition of CNTs shows a decrease in strength. The Young's modulus shows the same general trend as the strength. As shown in Fig. 6, the average modulus is less than the

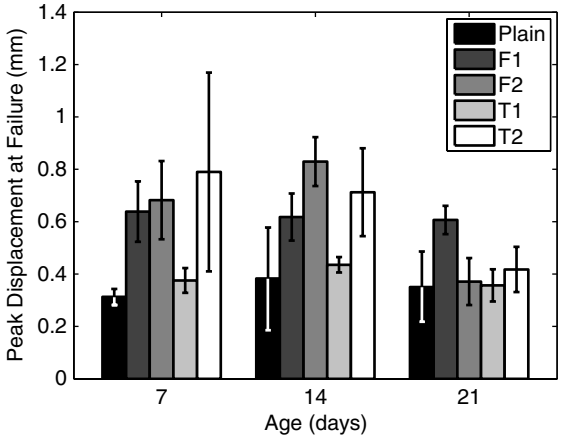

Fig. 4. Effect of the CNFs and MWCNTs on the strain capacity of cement paste

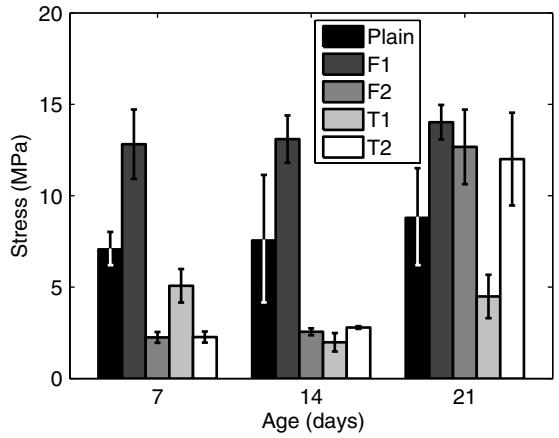

Fig. 5. Effect of the CNFs and MWCNTs on the ultimate strength of cement paste

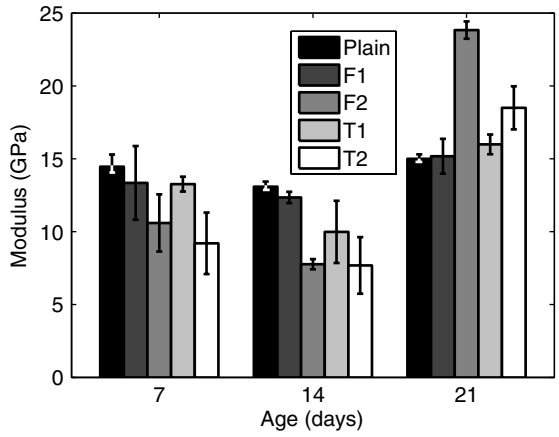

Fig. 6. Effect of the CNFs and MWCNTs on the elastic modulus of cement paste

reference sample at both 7 and 14 days. This delay in both strength and stiffness can also be attributed to a delay in the formation of high stiffness C-S-H at early ages. The toughness is calculated within MATLAB by simply integrating the area under the stress versus strain curve. From The greatest increase in fracture toughness (i.e., 270%) occurred at 7 days by F1 (Fig. 7).

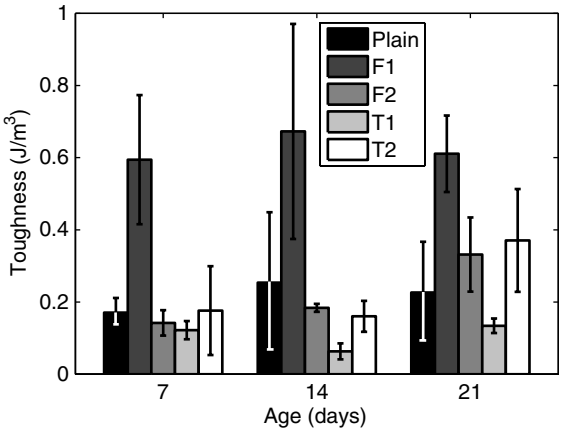

Fig. 7. Effect of the CNFs and MWCNTs on the fracture toughness of cement paste

The data for F2 and T2 show a close correlation with one another. Looking at the ultimate strength, elastic modulus, and fracture toughness, T2 and F2 both follow the same general trend. In general, the data presented in Figs. 4–7 show an increasing trend for strength, stiffness, and toughness, accompanied by a decrease in strain capacity. These trends are most likely attributable to the delay in the bonding mechanism between the nanofilaments and the cement paste.

Figs. 8–10 show samples with the highest strength from each batch at 7, 14, and 28 days, respectively. Out of all the 7 day samples, F1 had the highest load capacity, which is likely caused by the enhanced dispersion of the CNFs. T2 had the highest strain capacity. F1, T1, and the reference sample all had very similar stiffness measurements. For the 14 day test, F1 still had the highest load capacity. F2 also had the highest strain capacity. F1 and T2 were the only brittle failures. Of all samples tested at 28 days, the F2 batch had the highest strength and second highest strain capacity. F1 had the highest strain capacity and second highest strength. To date, this study is the first to present data for the fracture toughness behavior of nanofilament reinforced cementitious composites. At every age, F1 had a significantly higher toughness: a 73–265% increase above the plain cement. This increase in toughness is largely because of the CNFs ability to carry the load and absorb the energy as the cement matrix began to fracture. The following section

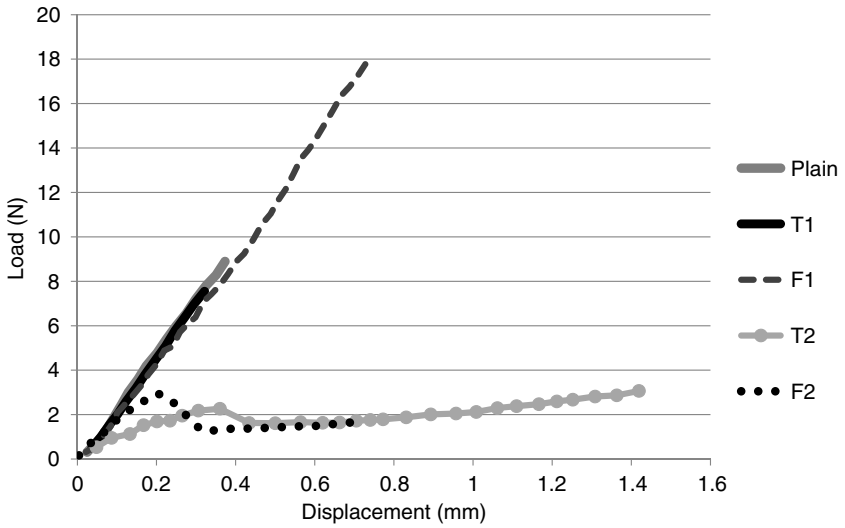

Fig. 8. Example of load-displacement response for the highest strength of each sample for the 7 day test

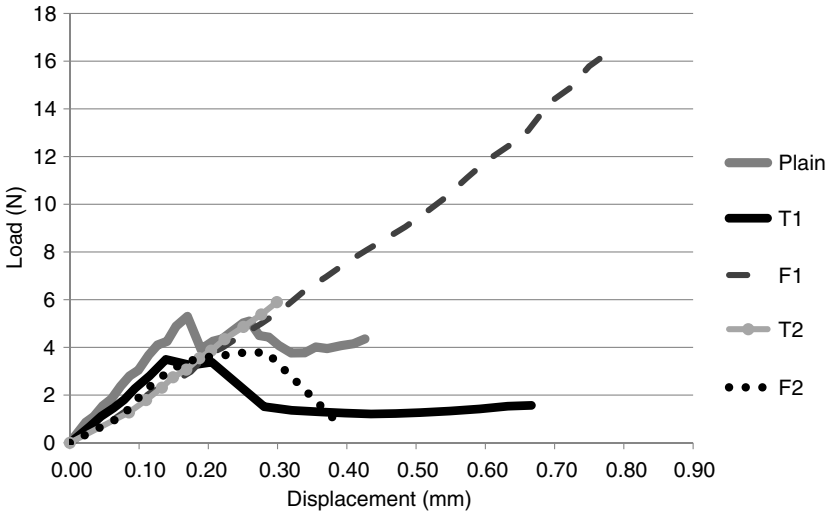

Fig. 9. Example of load-displacement response for the highest strength of each sample for the 14 day test

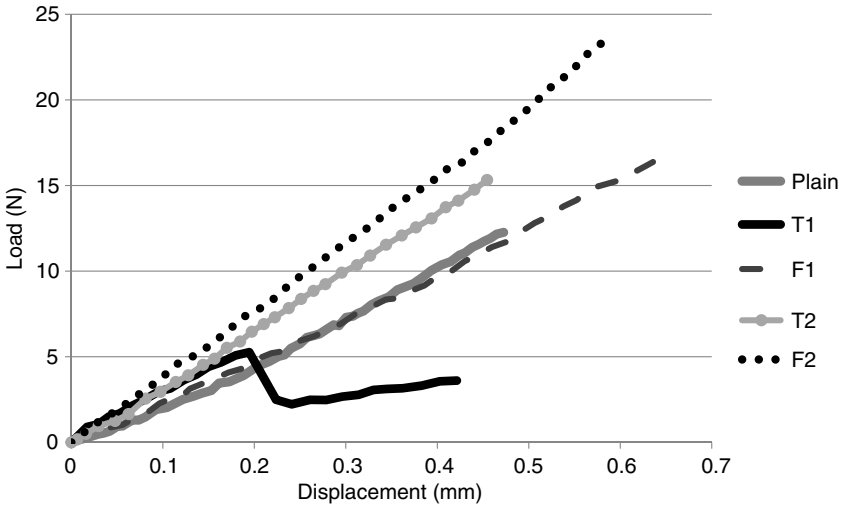

Fig. 10. Example of load-displacement response for the highest strength of each sample for the 28 day test

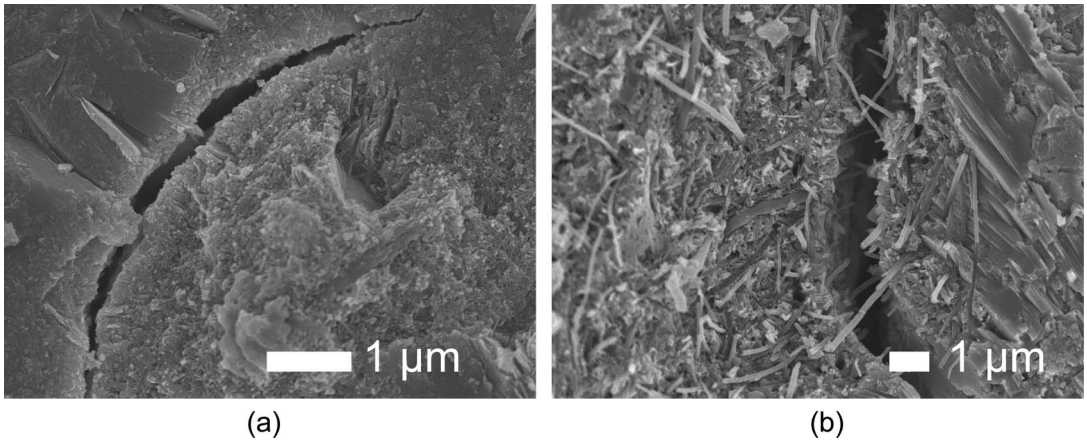

Fig. 11. (a) SEM image of the fractured surface with no CNFs within the region; (b) CNF bundled within a small area

outlines some of the microstructural observations that may explain most of the discrepancies in the obtained mechanical properties.

SEM Observation

Although CNTs or CNFs were well dispersed within the aqueous solution before mixing with the cement, the SEM observations of the fractured surface on the hardened cement containing either CNTs or CNFs show poor dispersion within the cement matrix. In fact, large areas observed under the SEM showed no evidence of either CNTs or CNFs. Despite the best efforts to maintain the dispersion of nanofilaments within the aqueous solution, combining a well-dispersed aqueous mixture with cement resulted in a relatively poor dispersion within the hydrated cement paste. Fig. 11(a) shows a typical SEM image. In the image, a crack is shown; however, no CNFs appeared anywhere within the region. On the other hand, Fig. 11(b) shows an area with a high concentration of CNFs. What causes the poor dispersion is unknown; however, the writers feel that the size and agglomeration of cement grains play a crucial role in the dispersion of nanofilaments within the cement matrix, as illustrated in Fig. 12.

Hard cement grains hydrate from the outside surface inward, toward the center. As the cement hydrates, areas that were previously hard cement grains absent of nano-filaments become

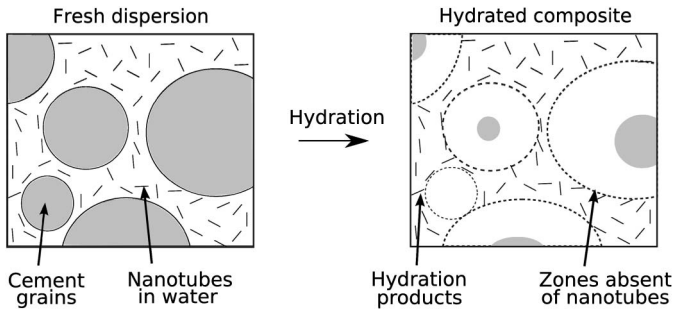

Fig. 12. Effect of cement grains on dispersibility of CNTs/CNFs; the large grains create zones that are absent of nanotubes/nanofibers even after hydration has progressed

hydrated C-S-H without any CNTs or CNFs. In certain cases, areas much greater than individual grains of cement were absent of nanofilaments as well. These areas were thought to contain no nanofilaments because the cement grains clumped together. For more details about the dispersion of CNTs and CNFs within the cement paste, see the research about dispersion issues within cementitious materials by Yazdanbakhsh et al. (2009).

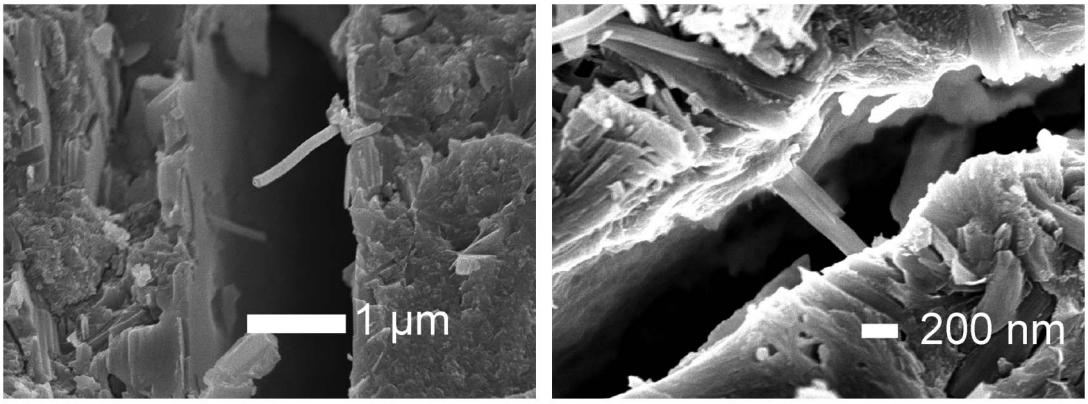

Fig. 13. (a) SEM image of a microcrack bridged by a CNF; (b) CNF pulled out from a microcrack

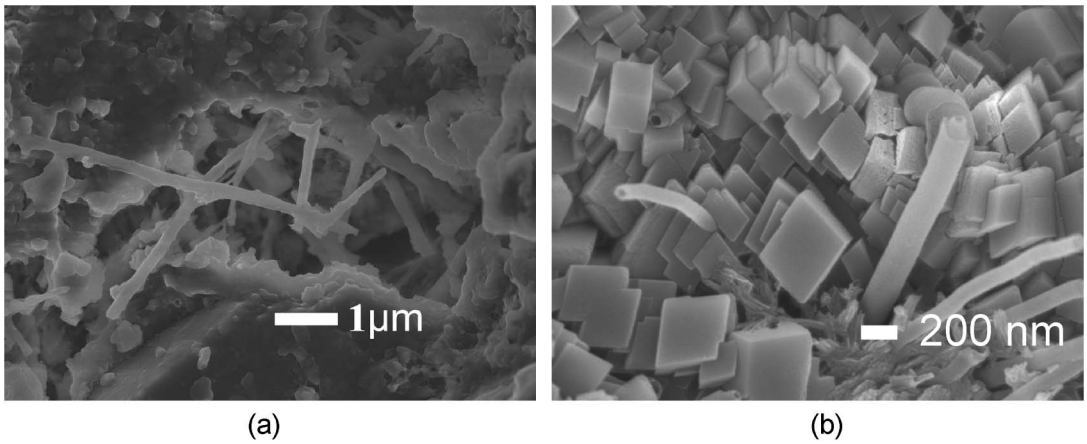

Fig. 14. (a) SEM image of treated CNFs embedded within the cement paste; (b) fractured end of a CNF protruding from the fractured surface of the cement

Fig. 13(a) shows a CNF bridging a microcrack, whereas the CNFs in Fig. 13(b) have been pulled out from the other wall. CNF and CNT pull-out was very common with SEM samples. In the writers' opinion, the untreated nanofilaments have a smooth surface for which the cement paste cannot properly develop a strong bond. One observation of this surface bonding is shown in Fig. 14. Fig. 14(b) shows functionalized CNFs embedded within cement paste. As shown in the figure, the functionalized CNFs have a surface coated with cement paste. Fig. 14(b) shows untreated CNFs within cement. In this image, a clear distinction can be made between the CNF and the cement surrounding it. No evidence of cement clinging to the surface of the CNF was observed. This indicates that the interfacial bond between cement and CNFs is weaker for the untreated CNFs than the acid treated CNFs.

Conclusions

The mechanical properties of cement paste samples reinforced with 0.1 and 0.2 wt% of CNTs or CNFs were investigated with a flexural test frame. The nanofilaments were dispersed with water and a surfactant by using an ultrasonic mixer, combined with cement having a 0.4 water to cement ratio, and poured into molds. The samples were allowed to cure for 7, 14, and 28 days and tested at each age. For almost all cases, the addition of CNFs and CNTs increased the peak displacement up to 150% higher than plain cement paste, which is crucial for structural applications in which higher ductility and strain capacity to failure is needed. For the early ages, 7 and 14 days, negative effects for the flexural strength, Young's modulus, and fracture toughness were observed; however, at 28 days, these properties increased beyond the plain cement, with the exception of F1. The F1 sample was able to outperform or match the plain cement sample in almost every category. SEM images verified poor dispersion within the cement paste matrix, the bridging effects, which transfer the load across the nano- and microcracks, and the fibers pull-out because of their weak bond.

A change between the aqueous dispersion and the final dispersion within the hydrated cement paste was observed. The change in dispersion was most likely because of the clumping of cement grains once added to the aqueous solution. These grains would hydrate while acting like a filter and not allowing the nanofilaments to pass among the grains. In turn, large areas on the fracture surface with few to no nanofilaments were observed, while other areas had large agglomerations.

The delayed enhancements in strength, ductility, and toughness, accompanied with a reduction in stiffness, were likely because of a shift in the bonding between the nanofilaments and the cement matrix. At early ages, 7 and 14 days, more nanofilaments pulled out, allowing for higher strain capacities. At the 28 day test, the bonding between nanofilaments and cement matrix increased to the point at which the nanofilaments were more susceptible to breaking rather than gradually pulling out. Moreover, generally, CNFs gave an improved performance because of their higher aspect ratio than CNTs. Future studies on the change in microstructural properties are

needed to fully understand how and why the cement composites show a delay in bond strength.

Acknowledgments

This study was sponsored in part by the Southwest University Transportation Center (SWUTC) through the U.S. Department of Transportation and also by the U.S. Federal Highway Administration through the cooperative agreement DTFH61-08-H-00004. The FE-SEM acquisition was supported in part by the National Science Foundation grant DBI-0116835, the Vice President for Research Office, and the Texas Engineering Experiment Station.

References

Altoubat, S., Yazdanbakhsh, A., and Rieder, K.-A. (2009). "Shear behavior of macro-synthetic fiber-reinforced concrete beams without stirrups." *ACI Mater. J.*, 106(4), 381–389.

Bandyopadhyaya, R., Nativ-Roth, E., Regev, O., and Yerushalmi-Rozen, R. (2002). "Stabilization of individual carbon nanotubes in aqueous solutions." *Nano Lett.*, 2(1), 25–28.

Chen, W., Auad, M. L., Williams, R. J. J., and Nutt, S. R. (2006). "Improving the dispersion and flexural strength of multiwalled carbon nanotubes-stiff epoxy composites through [beta]-hydroxyester surface functionalization coupled with the anionic homopolymerization of the epoxy matrix." *Eur. Polym. J.*, 42(10), 2765–2772.

Coleman, J. N., Khan, U., Blau, W. J., and Gun'ko, Y. K. (2006). "Small but strong: A review of the mechanical properties of carbon nanotube-polymer composites." *Carbon*, 44(9), 1624–1652.

Cwirzen, A., Habermehl-Cwirzen, K., and Penttala, V. (2008). "Surface decoration of carbon nanotubes and mechanical properties of cement/carbon nanotube composites." *Adv. Cem. Res.*, 20(2), 65–73.

Fischer, G., and Li, V. C. (2007). "Effect of fiber reinforcement on the response of structural members." *Eng. Fract. Mech.*, 74(1–2), 258–272.

Grunlan, C., Liu, L., and Regev, O. (2008). "Weak polyelectrolyte control of carbon nanotube dispersion in water." *J. Colloid Interface Sci.*, 317(1), 346–349.

Li, G. Y., Wang, P. M., and Zhao, X. (2005). "Mechanical behavior and microstructure of cement composites incorporating surface-treated multi-walled carbon nanotubes." *Carbon*, 43(6), 1239–1245.

Li, G. Y., Wang, P. M., and Zhao, X. (2007). "Pressure-sensitive properties and microstructure of carbon nanotube reinforced cement composites." *Cem. Concr. Compos.*, 29(5), 377–382.

Li, V. C., and Maalej, M. (1996). "Toughening in cement based composites —Part II: Fiber reinforced cementitious composites." *Cem. Concr. Compos.*, 18(4), 239–249.

Makar, J. M., and Beaudoin, J. J. (2004). "Carbon nanotubes and their application in the construction industry." *Proc., 1st Int. Symp. on Nanotechnology in Construction*, P. J. M. Bartos, J. J. Hughes, P. Trtik, and W. Zhu, eds., Royal Society of Chemistry, Paisley, Scotland, 331–341.

Makar, J. M., Margeson, J. C., and Luh, J. (2005). "Carbon nanotube/cement composite—Early results and potential applications." *Proc., 3rd Int. Conf. on Construction Materials: Performance, Innovation and Structural Implications*, The Univ. of British Columbia, Vancouver, BC, Canada, 1–10.

Mangat, P. S., Motamedi-Azari, M., and Shakor Ramat, B. B. (1984). "Steel fibre-cement matrix interfacial bond characteristics under flexure." *Int. J. Cem. Compos. Lightweight Concr.*, 6(1), 29–37.

Marrs, B., Andrews, R., and Pienkowski, D. (2007). "Multiwall carbon nanotubes enhance the fatigue performance of physiologically maintained methyl methacrylate-styrene copolymer." *Carbon*, 45(10), 2098–2104.

Musso, S., Tulliani, J.-M., Ferro, G., and Tagliaferro, A. (2009). "Influence of carbon nanotubes structure on the mechanical behavior of cement composites." *Compos. Sci. Technol.*, 69(11–12), 1985–1990.

Ostertag, C. P., Yi, C. K., and Vondran, G. (2001). "Tensile strength enhancement in interground fiber cement composites." *Cem. Concr. Compos.*, 23(4–5), 419–425.

Sáez de Ibarra, Y., Gaitero, J. J., Erkizia, E., and Campillo, I. (2006). "Aromic force microscopy and nanoindentation of cement pastes with nanotube dispersions." *Phys. Status Solidi A*, 203(6), 1076–1081.

Sanchez, F. (2009). "Carbon nanofiber/cement composites: Challenges and promises as structural materials." *Int. J. Mater. Struct. Integr.*, 3(2–3), 217–226.

Savastano, J. H., Warden, P. G., and Coutts, R. S. P. (2005). "Microstructure and mechanical properties of waste fibre-cement composites." *Cem. Concr. Compos.*, 27(5), 583–592.

Shah, S. P., Konsta-Gdoutos, M. S., Metaxa, Z. S., and Mondal, P. (2009). "Nanoscale modification of cementitious materials." *Proc., 3rd Int. Symp. on Nanotechnology in Construction: NICOM3*, Springer-Verlag, Berlin,125–130.

Wang, C., Li, K.-Z., Li, H.-J., Jiao, G.-S., Lu, J., and Hou, D.-S. (2008). "Effect of carbon fiber dispersion on the mechanical properties of carbon fiber-reinforced cement-based composites." *Mater. Sci. Eng. A*, 487(1–2), 52–57.

Wang, J. G., Fang, Z. P., Gu, A. J., Xu, L. H., and Liu, F. (2006a). "Effect of amino-functionalization of multi-walled carbon nanotubes on the dispersion with epoxy resin matrix." *J. Appl. Polym. Sci.*, 100(1), 97–104.

Wang, Y., Iqbal, Z., and Mitra, S. (2006b). "Rapidly functionalized, water-dispersed carbon nanotubes at high concentration." *J. Am. Chem. Soc.*, 128(1), 95–99.

Wansom, S., Kidner, N. J., Woo, L. Y., and Mason, T. O. (2006). "AC-impedance response of multi-walled carbon nanotube/cement composites." *Cem. Concr. Compos.*, 28(6), 509–519.

Xie, X.-L., Mai, Y.-W., and Zhou, X.-P. (2005). "Dispersion and alignment of carbon nanotubes in polymer matrix: A review." *Mater. Sci. Eng., R*, 49(4), 89–112.

Yazdanbakhsh, A., Grasley, Z., Tyson, B., and Abu Al-Rub, R. (2009). "Carbon nanofibers and nanotubes in cementitious materials: Some issues on dispersion and interfacial bond." *Special Publication V. SP 267*, ACI, Farmington Hills, MI, 21–34.

Yu, M. F., Lourie, O., Dyer, M. J., Moloni, K., Kelly, T. F., and Ruoff, R. S. (2000). "Strength and breaking mechanism of multiwalled carbon nanotubes under tensile load." *Science*, 287(5453), 637–640.

Zhao, B., Hu, H., Yu, A. P., Perea, D., and Haddon, R. C. (2005). "Synthesis and characterization of water soluble single-walled carbon nanotube graft copolymers." *J. Am. Chem. Soc.*, 127(22), 8197–8203.

Zhou, Z. P., et al. (2009). "Development of carbon nanofibers from aligned electrospun polyacrylonitrile nanofiber bundles and characterization of their microstructural, electrical, and mechanical properties." *Polymer*, 50(13), 2999–3006.